Second-harmonic generation with pulses in a coupled-resonator optical waveguide

Shayan Mookherjea*
Department of Electrical Engineering, 136-93 California Institute of Technology, Pasadena, California 91125

Amnon Yariv
Department of Applied Physics, 128-95 California Institute of Technology, Pasadena, California 91125

(Received 18 July 2001; revised manuscript received 3 October 2001; published 23 January 2002)

We describe the generation and propagation of pulses in a coupled-resonator optical waveguide driven by a nonlinear polarization using a method closely related to the coupled-mode theory. The specific example we consider is that of second-harmonic generation. This formalism explicitly accounts for temporal dependencies in the waveguide field distributions and in their representations in terms of slowly modulated Bloch wave functions, in contrast with the equations obtained previously for cw second-harmonic generation.

DOI: 10.1103/PhysRevE.65.026607 PACS number(s): 42.70.Qs, 42.65.Ky, 42.25.Bs

I. INTRODUCTION

A type of waveguide based on the coupling of optical resonators has been recently introduced, and is called the coupled resonator optical waveguide (CROW) [1]. As the name suggests, waveguiding in a CROW is achieved fundamentally not by total internal reflection or Bragg reflection from a periodic structure, but instead, by the overlap between the individual resonator modes of the structural elements that comprise the waveguide. In a two-dimensional (2D) photonic crystal, formed by etching a periodic array of air holes (of refractive index n_1) in a dielectric material (of refractive index n_2) [2], a CROW can be realized, as shown in Fig. 1, by coupling defect cavities as the individual resonators.

CROWs offer remarkable possibilities for optical component design. A CROW formed by weak coupling of high-Q individual resonator modes is characterized by a nearly flat dispersion relationship and potentially very low group velocity in the waveguide [1], which can be used for efficient cw second-harmonic generation [3]. Further, a weakly coupled CROW implies tight confinement of the optical power in the individual resonator modes, which leads to very high optical intensities even at moderate (propagating) power levels. This property, in conjunction with the low group velocity, can be utilized in a photorefractive CROW for holography of optical pulses with much lower intensities than in conventional dielectric waveguides, leading to the possibility of single-shot room-temperature optical pulse storage and readout [4].

The formalism used to analyze the waveguide modes in such structures is known as the tight-binding approximation in solid-state physics [5,6]. It describes electrons in a crystal with a strong periodic potential due to the lattice structure of localized atoms, characterized by a weak overlap between the atomic wave functions. By analogy, the optical structures that can be described using the tight-binding approximation are those that consist of isolated structural elements capable of supporting localized electromagnetic fields (e.g., high-Q resonators such as defect modes in photonic crystals [7]) weakly coupled to one another. In this case, the waveguide modes are closely related to the eigenmodes of the individual elements rather than to the complex-exponential eigenmodes of free-space propagation. Recent experiments in the microwave and optical regime have demonstrated the validity of the tight-binding approximation in a weakly coupled CROW structure [8,9].

Prior to [10], the analysis of field evolution in CROWs (and related structures) has been restricted to monochromatic waves at the eigenfrequencies of the waveguide. We have recently described the linear propagation of pulses with a nonzero spread of wave vectors, resulting in a closed-form expression for the electric field due to pulse propagation in a CROW, as shown in Fig. 2.

The analysis of [10] shows that the waveguide imposes limits on both the maximum and minimum temporal extent of the pulse. While the latter is a consequence of the spatial geometry of the waveguide, the limit on the maximum pulse duration is directly related to the finite length of the structure. Following the literature convention on second-harmonic generation in bulk crystals [11,12], we assume that the second-harmonic generation processes described in this paper take place over an essentially infinitely long waveguide.

This paper investigates how the nonlinear polarization generated in a CROW at the second-harmonic frequency (of a reference pulse) changes the amplitude of the waveguide

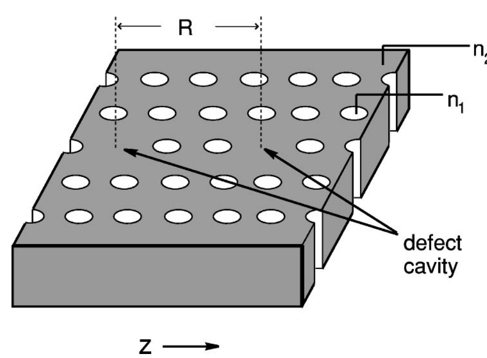

FIG. 1. Schematic of an infinitely long 1D CROW with periodicity R consisting of defect cavities embedded in a 2D photonic crystal.

*Electronic address: shayan@caltech.edu;
URL: http://www.its.caltech.edu/~shayan

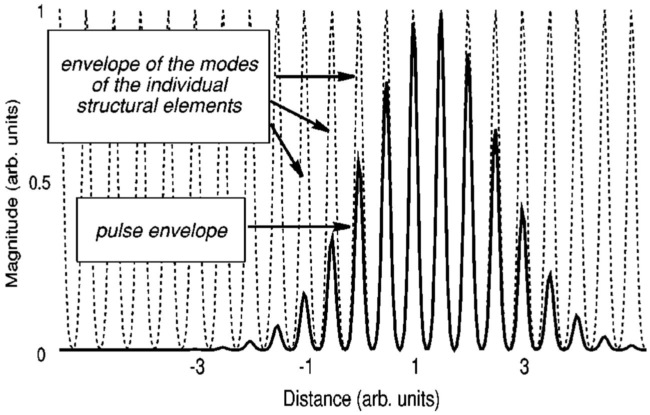

FIG. 2. The Gaussian envelope of a pulse propagating in a 1D CROW, with the envelope of the weakly coupled resonator eigenmodes shown by the dotted lines.

field distribution that describes a propagating pulse. In the CROW structures we investigate, pulses can propagate with very little distortion in their envelopes [10], and therefore, the effect of a pulse at one optical frequency on another at a different optical frequency can be treated in the same framework as the conventional coupled-mode theory of waveguide modes [11]. The reason for our interest in this phenomenon, aside from it being the most fundamental of (quasi-) nonlinear phenomena in the coupled-mode framework, is the following: the efficiency of (unsaturated) second-harmonic generation in a CROW with cw waves is enhanced relative to that in bulk crystals by the inverse ratio of the group velocities at the second harmonic frequency in the two waveguides [3], which can approach 10^3 or 10^4 for weakly coupled CROWs [1]. It is known that the efficiency of second-harmonic generation is enhanced at the band edge of photonic crystals, for exactly similar reasons of a reduction in the group velocity [13]. Second-harmonic generation in a CROW combines this advantage with the enhancement of the optical field found, e.g., in defect cavities in photonic crystals [14,15]. A numerical simulation of second-harmonic generation with pulses in related structures is presented in [16] and shows many similar features with our discussion.

A prefactory caveat: the tight-binding description of certain related structures such as deep superstructure Bragg gratings [17], may correctly assume that the individual resonator modes are nondegenerate. This is not strictly true for a CROW, but in this paper we will restrict our discussion to modes of a particular parity. If two degenerate single-resonator modes have opposite parity (as in the case of a defect cavity in a photonic crystal), they cannot couple to each other [3]. Consequently, the dispersion relationship (and group velocity) of the two CROW bands are identical.

II. WAVEGUIDE MODES

In a CROW comprising of weakly coupled identical high-Q resonators separated by a distance R, the electric field distribution $\mathbf{E}(\mathbf{r},t)$ describing a pulse propagating along the z axis at the optical carrier (angular) frequency ω and wavevector $\mathbf{k}$ is [10]

$$\mathbf{E}(\mathbf{r},t)=e^{i\omega t}\sum_n e^{-iknR}\boldsymbol{\psi}(\mathbf{r}-nR\mathbf{e}_z)\mathcal{E}\left[z=0,t-\frac{nR}{v}\right], \quad (1)$$

where $\boldsymbol{\psi}(\mathbf{r})$ is the individual resonator eigenmode, $\mathcal{E}(z=0,t)$ is the input pulse envelope, and v is the group velocity at $k=|\mathbf{k}|$. The sign convention in the t and z exponents follows that of Yariv [11]. This equation is a simple restatement of [[10], Eq. (16)], obtained by dropping the summation over l using the arguments discussed at the end of the previous section, and generalizing the spatial dependence of $\boldsymbol{\psi}$ to the three-vector of spatial coordinates $\mathbf{r}$. Since we consider infinitely long structures, we may further drop the summation over m in [[10], Eq. (16)] as the Born-von Karman boundary conditions no longer apply. The terminology ''input pulse envelope'' should not be taken too literally, since the structures we consider are infinitely long: it merely means that we focus on the field evolution along a section of an infinite waveguide, and the ''input'' refers to the field distribution at one edge of this structure, i.e., a boundary condition, as discussed in [10]. The precise mathematical meaning of this assumption is rather technical and is discussed at the end of Appendix A.

For an infinitely long CROW where the summation over n in Eq. (1) can be relabeled to $n\pm1$, $\mathbf{E}(\mathbf{r},t)$ satisfies the $(3+1)D$ Bloch theorem [5,11],

$$\mathbf{E}(\mathbf{r}+R\mathbf{e}_z,t+R/v)=e^{i\omega R/v}e^{-ikR}\mathbf{E}(\mathbf{r},t). \quad (2)$$

Consequently, the field can be written in the Bloch form,

$$\mathbf{E}(\mathbf{r},t)=e^{i\omega t}e^{-ik(\omega)z}\mathbf{u}_{k(\omega)}(\mathbf{r},t), \quad (3)$$

where $\mathbf{u}_{k(\omega)}(\mathbf{r},t)$ is a vector-valued function with the periodicity of the CROW ''lattice'' and can be written out explicitly as

$$\mathbf{u}_{k(\omega)}(\mathbf{r},t)=\sum_n e^{ik_\omega(z-nR)}\boldsymbol{\psi}(\mathbf{r}-nR\mathbf{e}_z)\mathcal{E}\left[z=0,t-\frac{nR}{v}\right]. \quad (4)$$

The propagation ''constant'' k and the Bloch wave function depend on the frequency ω through the dispersion relationship. Nevertheless, our writing the eigenmodes in the Bloch form Eq. (3), is mainly for notational convenience in Sec. III. Plane waves of the form $\exp(-ikz)$ are not eigenmodes of the CROW waveguide in the tight-binding analysis.

The Bloch wave function is normalized according to the following inner-product definition between the vector space of the Bloch wave function and its dual space,

$$\int \frac{dt}{T}\int d\mathbf{r}\,\epsilon(\mathbf{r})[\mathbf{u}_{k(\omega)}(\mathbf{r},t)]^*\mathbf{u}_{k(\omega)}(\mathbf{r},t)=1, \quad (5)$$

where the spatial integration extends over a unit cell and the temporal integration over the extent of the pulse envelope, with a characteristic time constant T. This ensures that Eq. (5) still represents an electromagnetic energy conservation relationship [18], and can be interpreted as yielding a time-averaged energy stored in a unit cell volume [19]. We will abbreviate the notation to an integration over the four-vector r.

Maxwell's equations imply that the waveguide field distribution satisfies the following equation [11,18]:

$$\nabla\times[\nabla\times\mathbf{E}]+\frac{\epsilon(\mathbf{r})}{c^2}\frac{\partial^2\mathbf{E}}{\partial t^2}=\mathbf{0}, \tag{6}$$

and substituting in the Bloch form Eq. (3) for $\mathbf{E}(\mathbf{r},t)$, we can write this as an eigenvalue problem [20] for the Bloch wavefunction $\mathbf{u}_{k(\omega)}(\mathbf{r},t)$,

$$\begin{aligned}H\mathbf{u}_{k(\omega)}\equiv&-k^2\mathbf{e}_z\times[\mathbf{e}_z\times\mathbf{u}_{k(\omega)}]+\nabla\times[\nabla\times\mathbf{u}_{k(\omega)}]\\&-ik[\mathbf{e}_z\times[\nabla\times\mathbf{u}_{k(\omega)}]+\nabla\times[\mathbf{e}_z\times\mathbf{u}_{k(\omega)}]]\\&+\frac{\epsilon(\mathbf{r})}{c^2}\left[\frac{\partial^2\mathbf{u}_{k(\omega)}}{\partial t^2}+i2\omega\frac{\partial\mathbf{u}_{k(\omega)}}{\partial t}\right]\\=&\frac{\omega^2}{c^2}\epsilon(\mathbf{r})\mathbf{u}_{k(\omega)}.\end{aligned} \tag{7}$$

Note that Eq. (6) is not an eigenvalue equation—central to stating the wave equation as an eigenvalue problem (in the variable ω) is the assumption of time-harmonic solutions, or the introduction of ω through a multiplicative term such as $\exp(i\omega t)$. On the other hand, the presence of ω in the definition of the operator H in Eq. (7) does not invalidate the interpretation of Eq. (7) as an eigenvalue equation for $\mathbf{u}_{k(\omega)}(\mathbf{r},t)$ [21].

It is straightforward to verify that the operator H is Hermitian (see Appendix A for an outline of the proof). As a consequence of the dispersion relationship in the waveguide [18], the eigenvalue ω^2/c^2 is parametrized by k, and we can use the Hellman-Feynman theorem [21],

$$\begin{aligned}\frac{d(w/c)^2}{dk}=&\int d^4r[\mathbf{u}_{k(\omega)}]^*[-2k\mathbf{e}_z\times[\mathbf{e}_z\times\mathbf{u}_{k(\omega)}]\\&-i\mathbf{e}_z\times[\nabla\times\mathbf{u}_{k(\omega)}]-i\nabla\times[\mathbf{e}_z\times\mathbf{u}_{k(\omega)}]]\\&+i\frac{2}{c^2}\frac{d\omega}{dk}\int d^4r\,\epsilon(\mathbf{r})[\mathbf{u}_{k(\omega)}]^*\frac{\partial\mathbf{u}_{k(\omega)}}{\partial t}.\end{aligned} \tag{8}$$

Recognizing that $d\omega/dk$ defines the group velocity v [11], Eq. (8) can be rewritten as

$$\begin{aligned}&v\left[\frac{2\omega}{c^2}-i\frac{2}{c^2}\int d^4r\,\epsilon(\mathbf{r})[\mathbf{u}_{k(\omega)}]^*\frac{\partial\mathbf{u}_{k(\omega)}}{\partial t}\right]\\&=\int d^4r[\mathbf{u}_{k(\omega)}]^*[-2k\mathbf{e}_z\times[\mathbf{e}_z\times\mathbf{u}_{k(\omega)}]\\&\quad-i\mathbf{e}_z\times[\nabla\times\mathbf{u}_{k(\omega)}]-i\nabla\times[\mathbf{e}_z\times\mathbf{u}_{k(\omega)}]].\end{aligned} \tag{9}$$

III. SECOND-HARMONIC GENERATION

The standard approach to second-harmonic generation in bulk crystals introduces an envelope for the waveguide mode at the second-harmonic frequency and accounts for the generation of this envelope as a consequence of the nonlinear polarization in the medium [11,12]. We will adopt a similar approach, taking the field distributions from the linear tight-binding equations, i.e., we do not consider second-harmonic generation of intrinsically nonlinear pulse shapes such as solitons in this analysis. In bulk crystals, the eigenmodes are usually of a simple form—$\exp[i(\omega t-kz)]$—and the resultant equations for both cw waves and slowly varying envelope pulses are derived in [12]. In a CROW, the eigenmodes are more complicated as seen in Eq. (1), but the analysis can be carried out on similar lines. We have shown that in a CROW, a single-envelope function $E(z)$ can be applied to the field describing a pulse as a whole [22]. We adopt an approach based on the Bloch representation Eq. (3) that can be applied to other types of field propagation and evolution problems, where the structure exhibits spatial or temporal variations and does not admit simple complex exponential eigenmodes.

As discussed in detail in [22], we may assume the following *Ansatz* describing a pulse at the second-harmonic (carrier) frequency 2ω,

$$\mathbf{E}_2(\mathbf{r},t)=E_2(z)e^{i2\omega t}e^{-ik_{2\omega}z}\mathbf{u}_{k(2\omega)}(\mathbf{r},t), \tag{10}$$

whose Bloch component follows Eq. (9) with ω replaced by 2ω, and using the symbol v_2 for the group velocity at the second-harmonic frequency.

The nonlinear polarization $\mathbf{P}_{\mathrm{NL}}(\mathbf{r},t)$ generates the second-harmonic field $\mathbf{E}_2(\mathbf{r},t)$ according to [11,12,18]

$$\nabla\times[\nabla\times\mathbf{E}_2]+\frac{\epsilon(\mathbf{r})}{c^2}\frac{\partial^2\mathbf{E}_2}{\partial t^2}=-\frac{1}{c^2}\frac{\partial^2}{\partial t^2}\mathbf{P}_{\mathrm{NL}}(\mathbf{r},t). \tag{11}$$

We use the slowly varying approximation [11,12] to neglect the second-order derivatives of the envelope,

$$\left|\frac{d^2E_2}{dz^2}\right|\ll k_{2\omega}\left|\frac{dE_2}{dz}\right|,\quad k_{2\omega}{}^2|E_2|. \tag{12}$$

The spatial derivatives can be written as

$$\begin{aligned}&\nabla\times[\nabla\times\mathbf{E}_2]\\&=e^{i2\omega t}e^{-ik(2\omega)z}\Bigg[i\frac{\partial E_2}{\partial z}\{-2k_{2\omega}\mathbf{e}_z\times[\mathbf{e}_z\times\mathbf{u}_{k(2\omega)}]\\&\quad-i\mathbf{e}_z\times[\nabla\times\mathbf{u}_{k(2\omega)}]-i\nabla\times[\mathbf{e}_z\times\mathbf{u}_{k(2\omega)}]\}\\&\quad+E_2\{-k_{2\omega}{}^2\mathbf{e}_z\times[\mathbf{e}_z\times\mathbf{u}_{k(2\omega)}]+\nabla\times[\nabla\times\mathbf{u}_{k(2\omega)}]\\&\quad-ik_{2\omega}(\mathbf{e}_z\times[\nabla\times\mathbf{u}_{k(2\omega)}]-i\nabla\times[\mathbf{e}_z\times\mathbf{u}_{k(2\omega)}])\}\Bigg]\end{aligned} \tag{13}$$

and the temporal derivatives can be written as

$$\frac{\partial^2 \mathbf{E}_2}{\partial t^2} = e^{i2\omega t} e^{-ik(2\omega)z} \left\{ E_2 \left[\frac{\partial^2 \mathbf{u}_{k(2\omega)}}{\partial t^2} + i2(2\omega) \frac{\partial \mathbf{u}_{k(2\omega)}}{\partial t} - (2\omega)^2 \mathbf{u}_{k(2\omega)} \right] \right\}. \tag{14}$$

We substitute Eqs. (13) and (14) in Eq. (11) and use the eigenvalue equation for $\mathbf{u}_{k(2\omega)}$ [analogous to Eq. (7)] to cancel certain terms. The result can be written as

$$\begin{aligned} i\frac{dE_2}{dz}[&-2k_{2\omega}\mathbf{e}_z \times [\mathbf{e}_z \times \mathbf{u}_{k(2\omega)}] - i\mathbf{e}_z \times [\boldsymbol{\nabla} \times \mathbf{u}_{k(2\omega)}] \\ &- i\boldsymbol{\nabla} \times [\mathbf{e}_z \times \mathbf{u}_{k(2\omega)}]] \\ &= e^{ik(2\omega)z} e^{-i2\omega t} \left[-\frac{1}{c^2} \right] \frac{\partial^2}{\partial t^2} \mathbf{P}_{\mathrm{NL}}(\mathbf{r},t). \end{aligned} \tag{15}$$

Next, we form the inner product of both sides of Eq. (15) with $\mathbf{u}^*_{k(2\omega)}$ and integrate over t and $\mathbf{r}$ as in Eq. (5). Using Eq. (9) at the second-harmonic frequency, the left-hand side of Eq. (15), which we write as $\mathcal{L}$, becomes

$$\mathcal{L} = i\frac{dE_2}{dz} v_2 \left[\frac{4\omega}{c^2} - i\frac{2}{c^2} \int d^4r\, \boldsymbol{\epsilon}(\mathbf{r}) [\mathbf{u}_{k(2\omega)}]^* \frac{\partial \mathbf{u}_{k(2\omega)}}{\partial t} \right]. \tag{16}$$

We simplify the right-hand side of Eq. (15) using Eq. (B7) if we may assume an undepleted fundamental, or using Eq. (B8) otherwise. The differences between the two cases are mostly notational and we will consider the former first. With the following definitions based on Eqs. (10) and (B1),

$$\Delta k_n \equiv k_1(\omega) + k_2(\omega) - k(2\omega) + n\frac{2\pi}{R},$$

$$\mathbf{p}(\mathbf{r},t) \equiv \mathbf{u}_{k_1(\omega)}(\mathbf{r},t-z/v_1)\mathbf{u}_{k_2(\omega)}(\mathbf{r},t-z/v_1), \tag{17}$$

forming the above-mentioned inner product of the right-hand side of Eq. (15), which we write as $\mathcal{R}$, yields

$$\mathcal{R} = -\frac{1}{c^2} E_1^2 \int d^4r\, e^{-i\Delta K_n z} e^{in(2\pi/R)z} [\mathbf{u}_{k(2\omega)}(\mathbf{r},t)]^* \cdot \tilde{d}(\mathbf{r}) \left[\frac{\partial^2 \mathbf{p}}{\partial t^2} + 2i(2\omega)\frac{\partial \mathbf{p}}{\partial t} + (i2\omega)^2 \mathbf{p} \right]. \tag{18}$$

From Eqs. (16) and (18), it is clear that E_2 will remain small unless there exists an integer n such that $\boldsymbol{\Delta} k_n$ is very small. Then, $\exp(-i\boldsymbol{\Delta} k_n z)$ is essentially constant over one unit cell and can be pulled out of the integral. Therefore,

$$\mathcal{R} = \frac{4\omega^2}{c^2} E_1^2 e^{-i\Delta k_n z} \left[D_n^{(0)} - i\frac{1}{\omega} D_n^{(1)} - \frac{1}{4\omega^2} D_n^{(2)} \right], \tag{19}$$

where

$$D_n^{(0)} \equiv \int d^4r\, e^{in(2\pi/R)z} [\mathbf{u}_{k_2(2\omega)}(\mathbf{r},t)]^* \cdot \tilde{d}(\mathbf{r}) \mathbf{u}_{k_1(\omega)}(\mathbf{r},t-z/v_1) \mathbf{u}_{k_2(\omega)}(\mathbf{r},t-z/v_1), \tag{20}$$

$$D_n^{(1)} \equiv \int d^4r\, e^{in(2\pi/R)z} [\mathbf{u}_{k_2(2\omega)}(\mathbf{r},t)]^* \cdot \tilde{d}(\mathbf{r}) \frac{\partial}{\partial t} [\mathbf{u}_{k_1(\omega)}(\mathbf{r},t-z/v_1) \mathbf{u}_{k_2(\omega)}(\mathbf{r},t-z/v_1)], \tag{21}$$

$$D_n^{(2)} \equiv \int d^4r\, e^{in(2\pi/R)z} [\mathbf{u}_{k_2(2\omega)}(\mathbf{r},t)]^* \cdot \tilde{d}(\mathbf{r}) \frac{\partial^2}{\partial t^2} [\mathbf{u}_{k_1(\omega)}(\mathbf{r},t-z/v_1) \mathbf{u}_{k_2(\omega)}(\mathbf{r},t-z/v_1)]. \tag{22}$$

To allow for variations in the envelope of the fundamental, we replace ${E_1}^2$ in Eq. (19) by $E_1(z)$. We write down the equation that describes the evolution of the envelope of the second-harmonic field (at the frequency 2ω) in its complete form for convenient reference,

$$\frac{dE_2}{dz}=\left[i\frac{4\omega}{c^2}+\frac{2}{c^2}\int d^4r\,\epsilon(\mathbf{r})[\mathbf{u}_{k(2\omega)}(\mathbf{r},t)]^*\cdot\frac{\partial}{\partial t}\mathbf{u}_{k(2\omega)}(\mathbf{r},t)\right]^{-1}\frac{4\omega^2}{v_2c^2}\exp\left[-i\left(k_1(\omega)+k_2(\omega)-k(2\omega)+n\frac{2\pi}{R}\right)z\right]$$
$$\times\left\{\int d^4r\,e^{in(2\pi/R)z}[\mathbf{u}_{k_2(2\omega)}(\mathbf{r},t)]^*\cdot\tilde{d}(\mathbf{r})E_1(z)^2\left[\mathbf{u}_{k_1(\omega)}(\mathbf{r},t-z/v_1)\mathbf{u}_{k_2(\omega)}(\mathbf{r},t-z/v_1)\right.\right.$$
$$-\frac{i}{\omega}\int d^4r\,e^{in(2\pi/R)z}[\mathbf{u}_{k_2(2\omega)}(\mathbf{r},t)]^*\cdot\tilde{d}(\mathbf{r})\frac{\partial}{\partial t}[\mathbf{u}_{k_1(\omega)}(\mathbf{r},t-z/v_1)\mathbf{u}_{k_2(\omega)}(\mathbf{r},t-z/v_1)]$$
$$\left.\left.-\frac{1}{4\omega^2}\int d^4r\,e^{in(2\pi/R)z}[\mathbf{u}_{k_2(2\omega)}(\mathbf{r},t)]^*\cdot\tilde{d}(\mathbf{r})\frac{\partial^2}{\partial t^2}[\mathbf{u}_{k_1(\omega)}(\mathbf{r},t-z/v_1)\mathbf{u}_{k_2(\omega)}(\mathbf{r},t-z/v_1)]\right]\right\}. \tag{23}$$

IV. DISCUSSION

A closed form solution of Eq. (23) under general conditions is not known, and may not always be necessary in view of the different time scales on the right-hand side of Eq. (23). For certain practical applications, it may be simplest to adopt a numerical evaluation procedure instead of attempting an analytical solution. In this paper, instead, we will discuss certain simplifications which can lead to closed form solutions and demonstrate a correspondence with known results in the theory of second harmonic generation with cw waves.

As expected, dropping the time dependence and setting all time derivatives to zero in Eq. (23) yields the equation for second-harmonic generation with cw fields. This is an ordinary differential equation for $E_2(z)$ and can be solved quite easily with the assumption of an undepleted constant envelope fundamental. For efficient growth of the second harmonic even at this level of simplification highlights the phase matching condition,

$$k(2\omega)=k_1(\omega)+k_2(\omega)+n\frac{2\pi}{R},\qquad n=0,\pm1,\pm2,\ldots, \tag{24}$$

which explicitly involves the Bloch wave "vector" $n2\pi/R$. The enhanced efficiency of second-harmonic generation in such a CROW structure is presented in [3].

Analytical time-dependent solutions may also be obtained under certain approximations. We will continue to assume that E_1 is constant (undepleted constant fundamental) and introduce the parameter $p\equiv1/(i2\omega)$. Using Eqs. (20)–(22), we can write Eq. (23) as

$$v_2\frac{dE_2}{dz}=-\frac{E_1^2}{2pv_2}\left[1+p\int d^4r\,\epsilon(\mathbf{r})[\mathbf{u}_{k(2\omega)}]^*\frac{\partial}{\partial t}\mathbf{u}_{k(2\omega)}\right]^{-1}\times e^{-i\Delta k_n}[D_n^{(0)}+2pD_n^{(1)}+p^2D_n^{(2)}]. \tag{25}$$

For reasonably well-behaved picosecond pulses at the second harmonic [see Eq. (4)], we may assume

$$\left|p\int d^4r\,\epsilon(\mathbf{r})[\mathbf{u}_{k(2\omega)}]^*\frac{\partial}{\partial t}\mathbf{u}_{k(2\omega)}\right|\ll1. \tag{26}$$

To see this, we refer to Eq. (4) and consider a Gaussian pulse centered at a second-harmonic frequency of 532 nm in a CROW, $\mathcal{E}_2(z=0,t)=\exp(-t^2/\tau^2)$ where the pulse width τ is 1 ps. Then, the left-hand side of Eq. (26) can be written as

$$\frac{1.8\times10^{-15}s}{(1\times10^{-12})^2s^2}\int\frac{dt}{T}2t\int d\mathbf{r}\,\epsilon(\mathbf{r})[\mathbf{u}_{k(2\omega)}]^*\mathbf{u}_{k(2\omega)}\leqslant\frac{1.8\times10^{-15}s}{(1\times10^{-12})^2s^2}2T \tag{27}$$

since the range of t integration in Eq. (5) is over a time scale T. For picosecond pulses, T is on the order of picoseconds, and therefore, the above number is on the order of 10^{-2} or smaller.

The dominant contribution to second-harmonic generation then follows the equation

$$\frac{dE_2^{(0)}}{dz}=-\frac{E_1^2}{2pv_2}e^{-i\Delta k_nz}[D_n^{(0)}+2pD_n^{(1)}+p^2D_n^{(2)}]. \tag{28}$$

Equation (28) can be integrated with the usual boundary condition $E_2^{(0)}(z=0)=0$,

$$E_2^{(0)}(z)=-i\left[\frac{\sin[\Delta k_nz/2]}{\Delta k_nz/2}\right]e^{-i\Delta k_nz/2}\times zE_1^2\frac{\omega}{v_2}\left[D_n^{(0)}-i\frac{1}{\omega}D_n^{(1)}-\frac{1}{4\omega^2}D_n^{(2)}\right]. \tag{29}$$

The phase-matching sine function in Eq. (29) is exactly analogous to the results of cw second-harmonic generation in bulk crystals, but with the definition of Δk_n following Eq. (24). The condition $\Delta k_n=0$ (for some n) is known as quasiphase matching [11], and reflects the important role of the waveguide geometry on the efficiency of nonlinear processes.

Equation (29) also shows that at the phase-matched condition, the intensity of the second harmonic $|E_2|^2$ grows quadratically with distance z, the intensity of the fundamental $|E_1|^2$ and, in regions where it is a constant, the nonlinearity coefficient $\tilde{d}$; these are features in common with the analysis of second-harmonic generation in bulk media [12]. This is expected since we have shown that both problems reduce to that of a spatial envelope modulating a Bloch wave function, which satisfies an eigenvalue equation (consequent of Maxwell's equations).

The linear growth of $E_2^{(0)}$ with z cannot persist indefinitely; the saturation effects may partially be accounted for by explicitly including the loss coefficient in the expression $\exp(-\Gamma_{2\omega}+i2\omega t)$ in place of $\exp(i2\omega t)$ in Eq. (10). It may be seen that Eq. (29) is valid in the regime $z \ll v_2/\Gamma_{2\omega}$ [3].

In this regime, we can compute the efficiency of second-harmonic generation by comparing the intensity at the second harmonic obtained from Eq. (29) to the power flux of the fundamental. The electromagnetic energy density for the fundamental as written in Eq. (B1) is $|E_1|^2\epsilon(\mathbf{r})\mathbf{u}_{k(\omega)}{}^*\mathbf{u}_{k(\omega)}$. The group velocity v_1 (the velocity of energy flow) is intuitively defined as the ratio of the average power flow P_ω to the time-averaged energy stored per unit length, so that

$$P_\omega = v_1 \int d^4r\, \epsilon[\mathbf{u}_{k(\omega)}]^*\mathbf{u}_{k(\omega)} = \frac{v_1}{R}|E_1|^2. \tag{30}$$

Using Eq. (29), and assuming that the process is phase matched,

$$P_{2\omega(z)}(z) = \frac{v_2}{R}\left| E_1^2 \frac{1}{v_1 v_2}\,\omega R P_\omega z\left[D_n^{(0)} - i\frac{1}{\omega}D_n^{(1)} - \frac{1}{4\omega^2}D_n^{(2)}\right]\right|^2. \tag{31}$$

From Eqs. (30) and (31), the second-harmonic generation efficiency at $z=L$ is

$$\eta(L) = \frac{P_{2\omega}}{P_\omega} = \frac{1}{v_1^2 v_2}\,\omega^2 R P_\omega L^2 \left| D_n^{(0)} - i\frac{1}{\omega}D_n^{(1)} - \frac{1}{4\omega^2}D_n^{(2)}\right|^2. \tag{32}$$

The factors of $1/{v_1}^2$ and $1/v_2$ show that the efficiency of second-harmonic generation is greatly increased by slowing down the propagation of pulses in the waveguide.

The equations describing sum-frequency generation in photonic crystal waveguides with time-independent envelopes has been formulated by Sakoda and Ohtaka and solved using a Green's function [23,24]. There are similarities between their analysis and those in [3], and with the time-independent limit of the formulation in this paper. The expression derived by Sakoda and Ohtaka for an "effective nonlinear susceptibility" in Eq. (19) of [23] is similar to Eq. (20) in this paper and their results in Eqs. (24) and (A7) of [23] are similar to Eq. (29). In particular, the enhancement of the field intensity by a factor $1/v^2$ as in Eq. (32) and the conservation of crystal momentum $\Delta k_n(z)=0$ are similar. We point out that in contrast with Appendix A of [23], plane waves are not eigenfunctions of a CROW and evaluation of the integrals in a Green's function approach to the problem in this paper may not be possible.

A numerical study of pulsed second-harmonic generation in certain one-dimensional periodic structures (dielectric stacks) was presented by Scalora *et al.* [16]. The principle difference in their structure from a CROW lies in the location of the dispersion curve in the band diagram: in the structure of Scalora *et al.*, pulses are tuned to the band edge, whereas in the case of the CROW shown in Fig. 1, the defect cavity modes lie within the bandgap, and pulse propagation results from the weak overlap of the spatial distributions of these eigenmodes [3].

Although the physics behind the observations is different, there are several common phenomena such as a large reduction in the group velocity of pulse propagation (when tuned to the appropriate part of the spectrum) and increased intensity inside the waveguide relative to free space. The plots of the "pump field eigenmode distribution" as numerically obtained by Scalora *et al.* ([16], Fig. 4) from numerical simulations also correspond closely to our theoretical formulation in [10], which contains an (MPEG) animation of linear pulse propagation in waveguides whose eigenmodes are defined by a tight-binding analysis. This is a direct consequence of the similarities in the geometrical structure of deep-grating photonic bandgap structures [17] and a one-dimensional CROW.

Scalora *et al.* show that in the context of the slowly varying envelope approximation as used here, the assumption of an undepleted fundamental is valid (i.e., negligible absorption is observed) and in this regime, the efficiency of second-harmonic generation is increased by orders of magnitude as predicted in Eq. (32). For certain aspects of the problem, numerical simulations offer insight not yet available from a theoretical investigation. As we have mentioned in Appendix A, the problem of coupling a pulse into or out of such a structure cannot be described as a Hermitian eigenvalue problem. Scalora *et al.* demonstrate via simulations the importance of the pulse width in coupling into such a structure—pulses with a spectral width larger than that of the transmission resonance at the band-edge experience little field intensity enhancement. It is not clear at present if the bandwidth limitations that arise from the discrete geometry of a CROW [10] are related to this phenomena.

V. SUMMARY

We have derived the equation governing the propagation and generation of a waveguide field at the second-harmonic frequency as a consequence of a nonlinear polarization induced in a CROW by a field at the fundamental frequency. The Bloch functions in the description of the waveguide fields satisfy an eigenvalue equation, and the coupling of the fields may be described by a coupled-mode theory analogous to the treatment of coupled dielectric waveguides.

The CROW geometry can be applied to a variety of physical realizations, such as superstructure Bragg gratings and photonic crystal waveguides. The present analytical study complements the approach of numerical simulations, and is based on a formalism that explicitly considers the temporal coordinate in the Bloch wave functions and envelopes. The procedure we have employed is relevant to structures that lack space-invariance or time-invariance symmetry, as long as the form of the eigenmodes are known (or a reasonable ansatz is imposed) and their propagation is governed by an eigenvalue equation with a Hermitian operator and appropriate boundary conditions.

We have derived an approximate but analytical expression for the efficiency of unsaturated second-harmonic generation. We have also shown how the characteristics of the second harmonic field in a CROW has certain features in common with the well-known results in the generation of the second harmonic via cw waves in bulk crystals; these follow from the specific form imposed by the physics on the *Ansatz* of the fields in such waveguides. A four-wave mixing problem in this framework is discussed in [4].

ACKNOWLEDGMENTS

This work was supported by the U.S. Office of Naval Research and the U.S. Air Force Office of Scientific Research.

APPENDIX A: OUTLINE OF THE PROOF OF THE HERMITICITY OF *H*

Using the following two vector identities,

$$\nabla\cdot(\mathbf{a}\times\mathbf{b})=\mathbf{b}\cdot(\nabla\times\mathbf{a})-\mathbf{a}\cdot(\nabla\times\mathbf{b}),$$

$$\mathbf{a}\cdot(\mathbf{b}\times\mathbf{c})=-(\mathbf{b}\times\mathbf{a})\cdot\mathbf{c}, \tag{A1}$$

it is easy to show that the the linear operator H defined in Eq. (7) is Hermitian, provided that the boundary conditions are of the appropriate form [20]. To show this explicitly for each of the six component terms of H as written in Eq. (7) is needlessly tedious, as all the necessary operations can be demonstrated by considering terms 3 and 4 of H. We will therefore show that the operator H' which is defined by

$$H'\mathbf{u}_{k(\omega)}\equiv -ik_\omega\{\nabla\times[\mathbf{e}_z\times\mathbf{u}_{k(\omega)}]+\mathbf{e}_z\times[\nabla\mathbf{u}_{k(\omega)}]\} \tag{A2}$$

is Hermitian, i.e., satisfies the following equality among inner products:

$$(\mathbf{u}_{k(\omega)},H'\mathbf{u}_{k(\omega)})=(H'\mathbf{u}_{k(\omega)},\mathbf{u}_{k(\omega)}) \tag{A3}$$

with the inner product definition following Eq. (5). The full operator H can be checked in a similar way.

If the following boundary condition holds:

$$\int\frac{dt}{T}\int d\mathbf{r}\,\epsilon(\mathbf{r})\nabla\cdot[(\nabla\times\mathbf{u}_{k(\omega)})\times\mathbf{u}^*_{k(\omega)}]=0, \tag{A4}$$

where the region of $\mathbf{r}$ integration is over a unit cell and the region of t integration is over temporal extent of the envelope, then using Eq. (A1),

$$\begin{aligned}(\mathbf{u}_{k(\omega)},H'\mathbf{u}_{k(\omega)})&=\int\frac{dt}{T}\int d\mathbf{r}[-ik_\omega\epsilon(\mathbf{r})][(\nabla\cdot\mathbf{u}_{k(\omega)})^*[\mathbf{e}_z\\&\quad\times\mathbf{u}_{k(\omega)}]-(\mathbf{e}_z\times\mathbf{u}_{k(\omega)})^*(\nabla\times\mathbf{u}_{k(\omega)})]\\&=\int\frac{dt}{T}\int d\mathbf{r}[-ik_\omega\epsilon(\mathbf{r})][-(\mathbf{e}_z\times[\nabla\\&\quad\times\mathbf{u}_{k(\omega)}])^*\mathbf{u}_{k(\omega)}-(\nabla\times[e_z\times\mathbf{u}_{k(\omega)}])^*\mathbf{u}_{k(\omega)}\\&=(H'\mathbf{u}_{k(\omega)},\mathbf{u}_{k(\omega)}).\end{aligned} \tag{A5}$$

For terms 5 and 6 of H as given by Eq. (7), the following boundary condition is needed:

$$\int d\mathbf{r}\,\epsilon(\mathbf{r})\left[[\mathbf{u}_{k(\omega)}]^*\left(\frac{\epsilon(\mathbf{r})}{c^2}\frac{\partial\mathbf{u}_{k(\omega)}}{\partial t}\right)\Bigg|_{t_-}^{t_+}\right]=0. \tag{A6}$$

Equations (A4) and (A6) are satisfied physically since the CROW is a spatially periodic structure and the pulse envelope goes to zero at both ends of the t integration.

Such boundary conditions assume that the problem of interest is physically completely contained in the CROW, i.e., problems of coupling a pulse into or out of a CROW of finite length cannot be described by Hermitian eigenvalue equations as the bilinear concomitant between the original differential equation and its Hermitian adjoint is no longer periodic [20]. In such circumstances, one can resort to direct numerical methods of analysis [25].

The imposition of closed boundary conditions in the temporal domain is a physical realistic approximation we have used in an attempt to keep the analysis in this paper from becoming excessively complicated. A more correct approach would allow the positive temporal boundary to go to infinity and impose appropriate Cauchy boundary conditions (value and slope specified) on the wave equation. Whereas Cauchy boundary conditions overspecify a closed boundary hyperbolic differential equation, they provide for a unique and stable solution to the open boundary problem [20].

APPENDIX B: NONLINEAR POLARIZATION FOR SECOND-HARMONIC GENERATION

We assume the following forms for two fields at the fundamental frequency ω:

$$\mathbf{E}_a(\mathbf{r},t)=E_1e^{i\omega t}e^{-ik_1(\omega)z}\mathbf{u}_{k_1(\omega)}(\mathbf{r},t)$$

$$\mathbf{E}_b(\mathbf{r},t)=E_1e^{i\omega t}e^{-ik_2(\omega)z}\mathbf{u}_{k_2(\omega)}(\mathbf{r},t). \tag{B1}$$

For each field, the frequency-domain (temporal Fourier transformed) field can be written as

$$\begin{aligned}\tilde{\mathbf{E}}(\mathbf{r},\Omega)&\equiv E_1\int dt\,e^{-i\Omega t}\mathbf{E}(\mathbf{r},t)\\&=E_1e^{-ik_1(\omega)z}\tilde{\mathbf{u}}_{k_1}(\mathbf{r},\Omega),\end{aligned} \tag{B2}$$

where we use the tilde to represent Fourier transformed fields.

The frequency-domain nonlinear polarization for second-harmonic generation at ω_2 is given by [11,12]

$$\tilde{\mathbf{P}}_{\mathrm{NL}}(\mathbf{r},\omega_2)=\tilde{d}(\mathbf{r})\int_{-\infty}^{\infty}d\Omega\,\tilde{\mathbf{E}}_a(\mathbf{r},\omega_2-\Omega)\tilde{\mathbf{E}}_b(\mathbf{r},\Omega), \tag{B3}$$

where $\tilde{d}$ is the effective second-order nonlinearity coefficient of the medium. Using Eq. (B2), Eq. (B3) can be written as

$$\begin{aligned}\tilde{\mathbf{P}}_{\mathrm{NL}}(\mathbf{r},\omega_2)&=\tilde{d}(\mathbf{r})E_1^2\int_{-\infty}^{\infty}d\Omega\,e^{-i[k_1(\omega_2-\Omega)+k_2(\Omega)]z}\tilde{\mathbf{u}}_{k_1}(\mathbf{r},\omega_2\\&\quad-\Omega-\omega)\tilde{\mathbf{u}}_{k_2}(\mathbf{r},\Omega-\omega).\end{aligned} \tag{B4}$$

The dispersion relationship between k and ω implies that we can expand $k(\omega)$ in a Taylor series about the central frequency of each pulse [11]. We retain terms up to the linear in ω to write

$$k_1(\omega_2-\Omega)=k_1+\left.\frac{dk}{d\omega}\right|_{\omega}(\omega_2-\Omega-\omega),$$

$$k_2(\omega)=k_2+\left.\frac{dk}{d\omega}\right|_{\omega}(\Omega-\omega). \tag{B5}$$

The group velocity at ω_1 is defined by the relation $1/v_1=(dk/d\omega)|_{\omega_1}$. The assumption of a linear dispersion relationship in a CROW is not as restrictive as one might expect based on ω-k curves for conventional waveguides. From the tight-binding analysis, the dispersion relationship for a weakly coupled CROW can be written as

$$\omega(k)=\Omega\left[1-\frac{\alpha}{2}+\kappa\cos(kR)\right], \tag{B6}$$

where Ω is the mode frequency of the individual resonators, $\Delta\alpha$ is an overlap integral and κ is a coupling coefficient. The group-velocity $d\omega/dk$ goes to zero at the edges of the Brillouin zone $k=0,\ \pm\pi/R$, but is approximately constant in the central portion of the zone, where the dispersion relationship is linear.

We can use Eq. (B5) in Eq. (B4) and take the inverse Fourier transform to write the nonlinear polarization in the time domain,

$$\begin{aligned}\mathbf{P}_{\rm NL}(\mathbf{r},t)&=\int\frac{d\omega_2}{2\pi}e^{i\omega_2 t}\tilde{\mathbf{P}}_{\rm NL}(\mathbf{r},\omega_2)\\&=\tilde{d}(\mathbf{r})E_1^2e^{-i(k_1-\omega/v_1)z}e^{-i(k_2-\omega/v_1)z}\int\frac{d\omega_2}{2\pi}e^{i\omega_2(t-z/v_1)}\int_{-\infty}^{\infty}d\Omega\,\tilde{\mathbf{u}}_{k_1}(\mathbf{r},\omega_2-\Omega-\omega)\tilde{\mathbf{u}}_{k_2}(\mathbf{r},\Omega-\omega)\\&=\tilde{d}(\mathbf{r})E_1^2[e^{i(\omega t-k_1 z)}\mathbf{u}_{k_1(\omega)}(\mathbf{r},t-z/v_1)][e^{i(\omega t-k_2 z)}\mathbf{u}_{k_2(\omega)}(\mathbf{r},t-z/v_1)].\end{aligned} \tag{B7}$$

This can be easily generalized to include a spatial dependency in the envelope E_1. We can simply include the nonconstant part of E_1 with the spatially (and temporally) varying function $\mathbf{u}_{k(\omega)}(\mathbf{r},t)$ as the physical interpretation of $\mathbf{u}_{k(\omega)}$ as a Bloch wave function is irrelevant here. The result is

$$\mathbf{P}_{\rm NL}(\mathbf{r},t)=\tilde{d}(\mathbf{r})[E_a(z)e^{i(\omega t-k_1 z)}\mathbf{u}_{k_1(\omega)}(\mathbf{r},t-z/v_1)][E_b(z)e^{i(\omega t-k_2 z)}\mathbf{u}_{k_2(\omega)}(\mathbf{r},t-z/v_1)]. \tag{B8}$$

In this paper, we will assume for simplicity that the envelopes E_a and E_b are constant $=E_1$, signifying an undepleted field at the fundamental frequency ω.

[1] A. Yariv, Y. Xu, R. Lee, and A. Scherer, Opt. Lett. **24**(11), 711 (1999).

[2] J. Joannopoulos, R. Meade, and J. Winn, *Photonic Crystals* (Princeton University Press, Princeton, NJ, 1995).

[3] Y. Xu, R. Lee, and A. Yariv, J. Opt. Soc. Am. B **17(3)**, 387 (2000).

[4] S. Mookherjea and A. Yariv, Phys. Rev. E **64**, 066602 (2001).

[5] N. Ashcroft and N. Mermin, *Solid State Physics* (Harcourt Brace Jovanovitch, San Diego, 1976).

[6] R. Smith, *Wave Mechanics of Crystalline Solids* (Chapman and Hall, London, 1969).

[7] *Confined Electrons and Photons: New Physics and Applications*, Vol. 340 of *NATO Advanced Science Institute, Series B: Physics*, edited by E. Burnstein and C. Weisbuch (Plenum, New York, 1993).

[8] M. Bayindir, B. Temelkuran, and E. Ozbay, Phys. Rev. Lett. **84(10)**, 2140 (2000).

[9] S. Olivier, C. Smith, M. Rattier, H. Benisty, C. Weisbuch, T. Krauss, R. Houdré, and U. Oesterlé, Opt. Lett. **26**, 1019 (2001).

[10] S. Mookherjea and A. Yariv, Opt. Express **9**, 91 (2001).

[11] A. Yariv, *Optical Electronics in Modern Communications*, 5th ed. (Oxford University Press, New York, 1997), pp. 319–322.

[12] Y. Shen, *The Principles of Nonlinear Optics* (Wiley, New York, 1984).

[13] K. Sakoda, Opt. Express **4**, 167 (1999).

[14] P. Villeneuve, S. Fan, and J. Joannopoulos, Phys. Rev. B **54**, 7837 (1996).

[15] O. Painter, J. Vučković, and A. Scherer, J. Opt. Soc. Am. B **16**, 275 (1999).

[16] M. Scalora, M. Bloemer, A. Manka, J. Dowling, C. Bowden, R. Viswanathan, and J. Haus, Phys. Rev. A **56**, 3166 (1997).

[17] C. M. de Sterke, Phys. Rev. E **57**(3), 3502 (1998).

[18] J. Jackson, *Classical Electrodynamics*, 3rd ed. (Wiley, New York, 1999).

[19] S. Ramo, J. Whinnery, and T. Van Duzer, *Fields and Waves in Communication Electronics*, 3rd ed. (Wiley, New York, 1994), pp. 404 and 405.

[20] P. Morse and H. Feshbach, *Methods of Theoretical Physics* (McGraw-Hill, New York, 1953).

[21] C. Cohen-Tannoudji, B. Diu, and F. Laloë, *Quantum Mechanics* (Hermann, Paris, 1977), pp. 1192–1193.

[22] S. Mookherjea and A. Yariv (unpublished).

[23] K. Sakoda and K. Ohtaka, Phys. Rev. B **54(8)**, 5742 (1996).

[24] K. Sakoda and K. Ohtaka, Phys. Rev. B **54(8)**, 5732 (1996).

[25] Y. Xu, R. Lee, and A. Yariv, Opt. Lett. **25(10)**, 755 (2000).